Journal of Nuclear Materials 389 (2009) 85–88

Contents lists available at ScienceDirect

Journal of Nuclear Materials

journal homepage: www.elsevier.com/locate/jnucmat

Effect of Nd and Pr addition on the thermal and mechanical properties of $(U,Ce)O_2$

Ken Kurosaki [a,*], Kosuke Tanaka [b], Masahiko Osaka [b], Hiroaki Muta [a], Masayoshi Uno [a], Shinsuke Yamanaka [a]

[a] Graduate School of Engineering, Osaka University, 2-1 Yamadaoka, Suita Osaka 565-0871, Japan
[b] Japan Atomic Energy Agency, Oarai-machi, Ibaraki 311-1393, Japan

A B S T R A C T

The thermal conductivity, Young's modulus, and hardness of $(U_{0.65-x}Ce_{0.3}Pr_{0.05}Nd_x)O_2$ ($x = 0.01$, 0.08, 0.12) were evaluated and the effect of Pr and Nd addition on the properties of $(U, Ce)O_2$ were studied. The polycrystalline high-density pellets were prepared with solid state reactions of UO_2, CeO_2, Pr_2O_3, and Nd_2O_3. We confirmed that all Ce, Pr, and Nd dissolved in UO_2 and formed solid solutions of $(U,Ce,Pr,Nd)O_2$. We revealed that the thermal conductivity of $(U_{0.65-x}Ce_{0.3}Pr_{0.05}Nd_x)O_2$ ($x = 0.12$) was up to 25% lower than that of $x = 0.01$ at room temperature. The Young's modulus of $(U_{0.65-x}Ce_{0.3}Pr_{0.05}Nd_x)O_2$ decreased with x, whereas the hardness values were constant in the investigated x range.

1. Introduction

Recently, an advanced fast reactor fuel concept has been proposed, in which uranium–plutonium mixed oxide (MOX) fuels containing certain amounts of fission products (FPs) and minor actinides (MAs) are irradiated up to very high-burnups: 150 GWd/t for average burnup [1–3]. We call such a fuel as a low decontamination fuel. There are a lot of advantageous of the low decontamination fuel, such as reduction of environmental burdens, effective use of resources, high proliferation resistance, and simple processes. However, in order to put into practical use of the fuel, the fuel behavior under irradiation should be clarified.

In the high-burnup low decontamination fuel, large quantities of FPs and MAs exist and they will have much effect on the fuel performance. It is well known that some FPs and MAs dissolve in the fuel matrix and form solid solutions of $(U,Pu,MAs,FPs)O_2$ and others form oxide or metallic inclusions and precipitate on the fuel matrix [4,5]. Especially, the dissolved FPs and MAs would affect directly the thermal and the mechanical properties of the fuel. Therefore, the purpose of the present study is to fabricate the pellets of $(U,Ce,Pr,Nd)O_2$ and to perform thermal and mechanical characterizations with the aim of clarifying the effect of Nd and Pr addition on various properties of $(U,Ce)O_2$ which is a simulated material of the MOX fuel. Here, Pr is a substitute for MAs, because the ionic radii of Pr and Am are similar [6] and Pr could exist in the tetravalent state as well as the trivalent state, like Am. On the other hand, Nd is the representative of all rare-earth fission products.

In the present paper, we will show the characterization results of $(U_{0.65-x}Ce_{0.3}Pr_{0.05}Nd_x)O_2$ ($x = 0.01$, 0.08, 0.12). We studied the effect of Nd and Pr addition on the thermal and mechanical properties of $(U,Ce)O_2$. The results obtained here would be useful for us in evaluating the performance of low decontamination fuels in fast reactors under high-burnups.

2. Experiment

We prepared three compositions of the fuel pellets: $(U_{0.65-x}Ce_{0.3}Pr_{0.05}Nd_x)O_2$ ($x = 0.01$, 0.08, 0.12). The Nd content was determined by a burnup calculation; the Nd content $x = 0.01$, 0.08, and 0.12 correspond to the burnup of 0, 150, and 250 GWd/t, respectively. Appropriate amounts of UO_2, CeO_2, Pr_2O_3, and Nd_2O_3 powders were mixed and pressed into green pellets under a uniaxial pressure of 150 MPa, followed by reacting and sintering at 1873 K under a reducing atmosphere.

To examine the phase states and determine the lattice parameter of the matrix phase, we collected powder X-ray diffraction (XRD) data on a diffractometer (RINT2000, RIGAKU) with Cu $K\alpha$ radiation in air at room temperature. The sample microstructure was observed by using a scanning electron microscope (SEM). The chemical composition of the samples was determined using an energy-dispersive X-ray (EDX) analysis. The sample density was calculated from the sample size and weights at room temperature.

The thermal conductivity (κ) was calculated from the heat capacity (C_P), thermal diffusivity (α), and density (d) using the following relationship [7]:

$$\kappa = \alpha C_P d. \quad (1)$$

The C_P data were estimated from the data of the constituent chemical forms of the samples reported in the database [8]. The thermal

* Corresponding author. Tel.: +81 6 6879 7905; fax: +81 6 6879 7889.
E-mail address: kurosaki@see.eng.osaka-u.ac.jp (K. Kurosaki).

0022-3115/$ - see front matter © 2009 Elsevier B.V. All rights reserved.
doi:10.1016/j.jnucmat.2009.01.011

diffusivity was measured by the laser flash method from room temperature to 1673 K in a vacuum (10^{-4} Pa).

Hardness (H) and Young's modulus (E) were determined by indentation tests using a dynamic ultra-microhardness tester (DUH-211S, Shimadzu) at room temperature. The maximum load was chosen to be 10, 20, 50, 100, 200, 500, and 1000 mN under a loading/unloading time of 10 s. Although the mechanical properties determined from the load-displacement curve would be influenced not only by the maximum load but also by the holding time, we performed the indentation test under the holding time to be zero. For a particular load, at least 50 indentation tests were conducted on the sample to increase the reliability of the experimental results. Methods for determining H and E through the indentation test are reported elsewhere [9]. The Vickers hardness was also measured using a Vickers hardness tester (MHT-1, Matsuzawa) at room temperature under the maximum load of 9800 mN.

3. Results and discussion

The XRD patterns of the samples are shown in Fig. 1, together with the peak positions of UO_2 [10]. In all the XRD patterns, there were no peaks derived from impurities, only the peaks corresponding to the CaF_2 type structure were detected. Therefore, in the present study, all Ce, Pr, and Nd dissolved in UO_2. We succeeded preparing single phase $(U,Ce,Pr,Nd)O_2$ solid solutions. From the powder XRD patterns, the cubic lattice parameter was calculated as summarized in Table 1. The lattice parameter decreased with increasing the Nd content.

The pellet densities calculated from the weight and dimensions are summarized in Table 1. We prepared two kinds of pellets: column shaped pellets for mechanical properties characterizations and disk shaped pellets for thermal conductivity measurements. The column shaped pellets exhibited relatively high densities (around 92% of the theoretical density: TD), whereas the densities of the disk shaped pellets were not so high (around 83%TD). The densities were almost the same regardless of the Nd content.

The SEM images of the column shaped pellets are shown in Fig. 2. The SEM images revealed that the grain size was few dozens of micro-meters and there were not much differences among the samples in the grain size. From the EDX analysis, we confirmed that the compositions of the products did not deviate a lot from the starting compositions.

The thermal diffusivity and conductivity of the samples are shown in Fig. 3, as a function of temperature. Since the sample densities were quite low, the thermal conductivity data were corrected to the values for fully dense pellets with 100%TD by using the following equation [11]:

$$\kappa_0 = \kappa_P \frac{1+\beta P}{1-P}, \tag{2}$$

where κ_p is the measured thermal conductivity with certain porosities, κ_0 is the corrected thermal conductivity for fully dense pellets, P is the porosity, and β is a constant (= 0.5). We confirmed that both the thermal diffusivity and conductivity decreased with temperature and the Nd content up to around 800 K, and they kept constant values at higher temperatures. These results implied that Ce, Pr, Nd dissolved in UO_2 acted as centers of phonon scattering. The same tendencies have been reported previously [12]. The thermal conductivity of $(U_{0.65-x}Ce_{0.3}Pr_{0.05}Nd_x)O_2$ (x = 0.12) was up to 25% lower

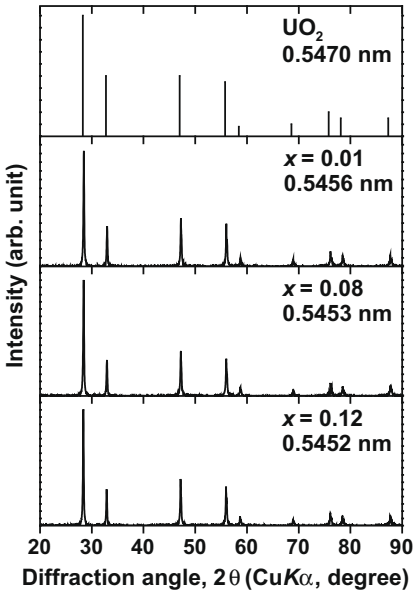

Fig. 1. XRD patterns of $(U_{0.65-x}Ce_{0.3}Pr_{0.05}Nd_x)O_2$ (x = 0.01, 0.08, 0.12), together with the peak position of UO_2.

Table 1
Sample characteristics of $(U_{0.65-x}Ce_{0.3}Pr_{0.05}Nd_x)O_2$ (x = 0.01, 0.08, 0.12).

		x = 0.01	x = 0.08	x = 0.12
Lattice parameter	(nm)	0.5456	0.5453	0.5452
Density of the column shaped pellets	(g/cm^3)	8.98	8.55	8.54
	(%TD)	93.4	91.3	92.8
Density of the disk shaped pellets	(g/cm^3)	7.88	7.77	7.78
	(%TD)	82.0	83.0	84.5

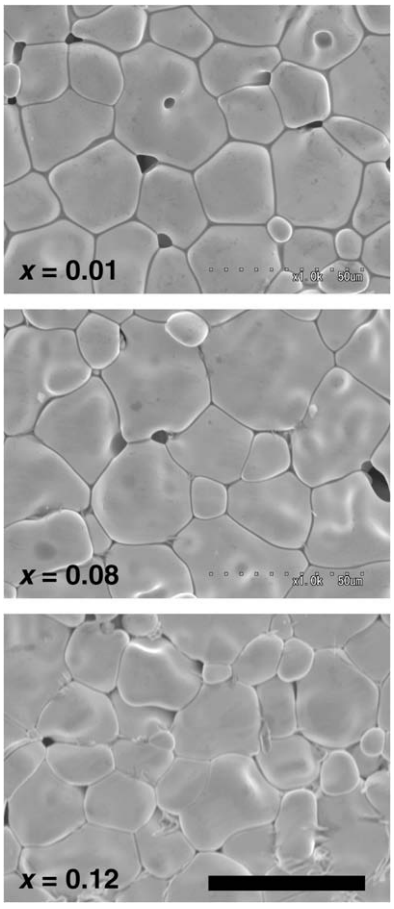

Fig. 2. SEM images of $(U_{0.65-x}Ce_{0.3}Pr_{0.05}Nd_x)O_2$ (x = 0.01, 0.08, 0.12). The scale bar is 50 μm.

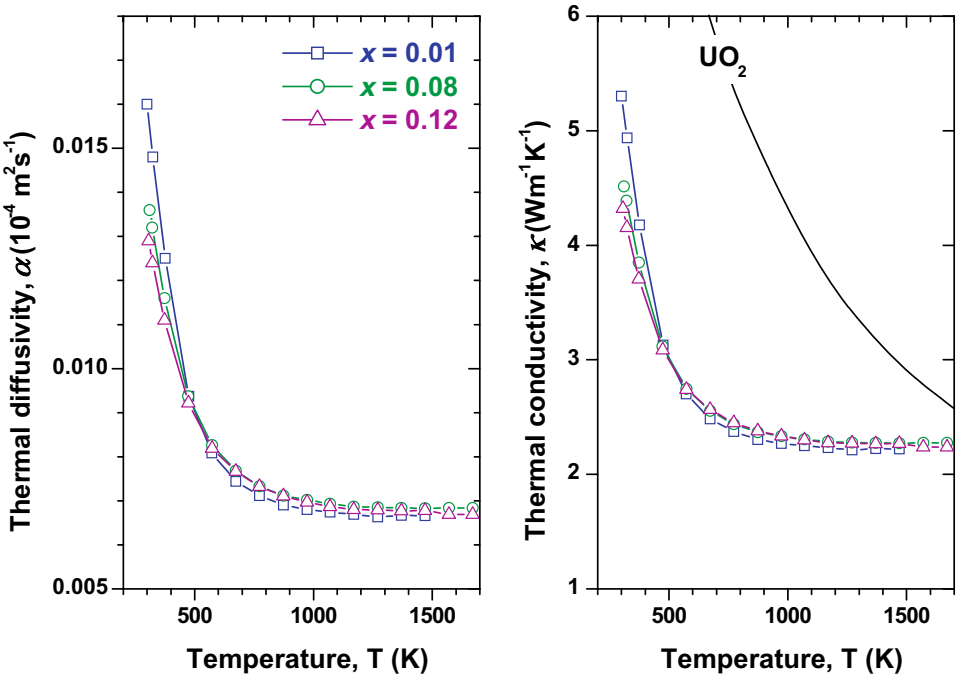

Fig. 3. Temperature dependence of the thermal diffusivities and conductivities of $(U_{0.65-x}Ce_{0.3}Pr_{0.05}Nd_x)O_2$ (x = 0.01, 0.08, 0.12), together with the data of UO_2.

than that of x = 0.01 at room temperature. In addition, the thermal conductivities of all samples were reduced approximately half of that of UO_2. These results mean that accumulation of FPs and MAs in the high-burnup MOX fuels significantly reduces the thermal conductivity.

Fig. 4 shows the Young's modulus of the pellets as a function of the indentation load. Clearly, the Young's modulus of all samples increased with decreasing the indentation load. And the values seem to decrease with increasing the Nd content, x.

Fig. 5 shows the hardness of the samples as a function of the indentation load. Clearly, the hardness of all samples increased with decreasing the indentation load, as in the case of the Young's modulus. However, all samples indicated similar hardness values, independent of the Nd content.

The decrease of load might reduce the probability of contact between the indenter and the sample's microscale pores, cracks, and grain boundaries. Such kind of contact would affect the load-displacement curve and lead to lower mechanical properties. In other words, it can be considered that the Young's modulus and hardness at infinitely small load could be considered as an intrinsic Young's modulus (E_0) and hardness (H_0) with no influences of sample's microstructures. We roughly determined the E_0 and H_0 for all samples by extrapolating the experimental data to that at the load equals to zero. Fig. 6 shows the E_0 and H_0 as a function of the Nd content. Apparently, the E_0 decreased with increasing the Nd content, while the hardness values of the samples were comparable, independent of the Nd content. We obtained the following empirical equation to describe the relationship between the E_0 and x.

$$E_0 = 269 - 556x (0.01 \leqslant x \leqslant 0.12) \quad (3)$$

Similar results were observed in similar materials: $(U,Ce,Nd)O_2$, in which the Young's modulus also decreased with the Nd content [13].

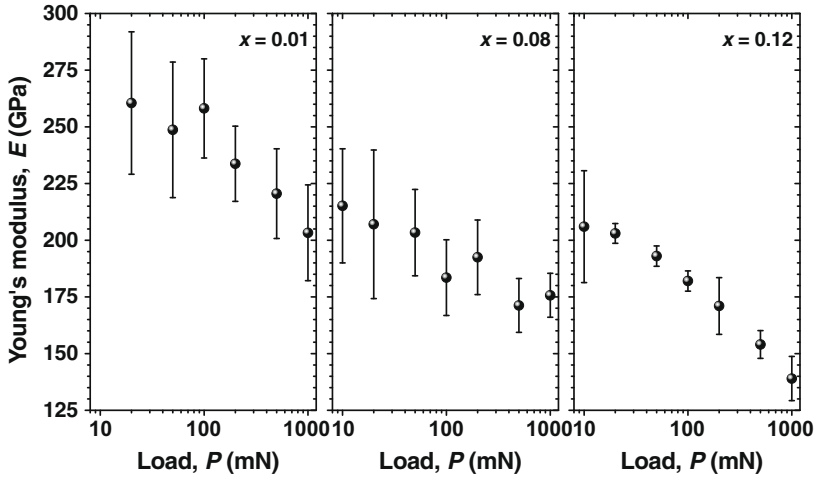

Fig. 4. Young's modulus of $(U_{0.65-x}Ce_{0.3}Pr_{0.05}Nd_x)O_2$ (x = 0.01, 0.08, 0.12), as a function of indentation load.

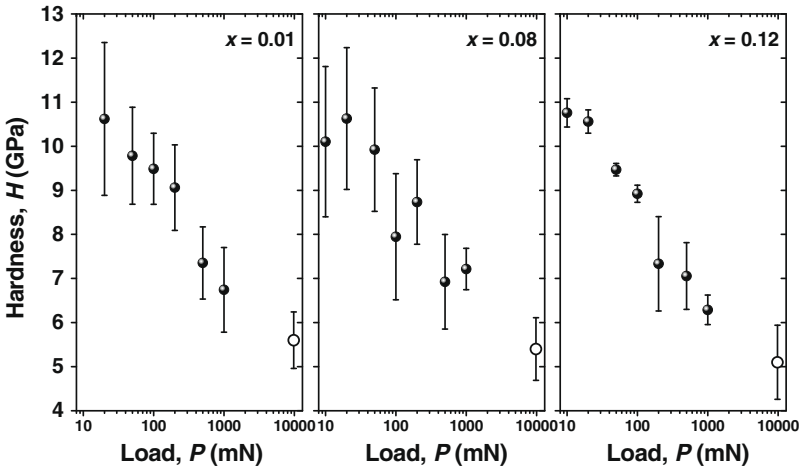

Fig. 5. Hardness of $(U_{0.65-x}Ce_{0.3}Pr_{0.05}Nd_x)O_2$ ($x = 0.01, 0.08, 0.12$), as a function of indentation load. The solid marks represent the results obtained from the indentation tests and the open marks represent the results obtained from the Vickers hardness tests.

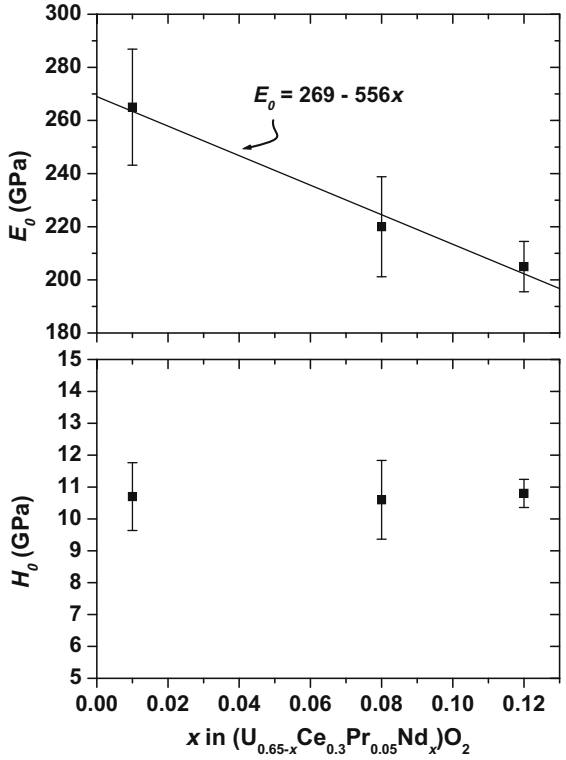

Fig. 6. Intrinsic Young's modulus (E_0) and hardness (H_0) of $(U_{0.65-x}Ce_{0.3}Pr_{0.05}Nd_x)O_2$ ($x = 0.01, 0.08, 0.12$), as a function of the Nd content, x.

4. Summary

In order to reveal the effect of Nd and Pr addition on the thermal and mechanical properties of $(U,Ce)O_2$, we prepared $(U_{0.65-x}Ce_{0.3}Pr_{0.05}Nd_x)O_2$ ($x = 0.01, 0.08, 0.12$) and evaluated the thermal conductivity, Young's modulus, and hardness. We succeeded preparing complete solid solutions of $(U,Ce,Pr,Nd)O_2$ with no impurities. The thermal conductivity of $(U_{0.65-x}Ce_{0.3}Pr_{0.05}Nd_x)O_2$ decreased with increasing the Nd content, indicating that Nd acted as centers of phonon scattering. The Young's modulus also decreased with increasing the Nd content, whereas the hardness were constant in the investigated compositions. These results would be useful in evaluating performance of high-burnup low decontamination fuel with large quantities of FPs and MAs.

Acknowledgments

Present study includes the result of "Study on the physical properties of nuclear fuels with multi phase system: Toward establishment of the closed cycle system with low-decontaminated oxide fuel" entrusted to Osaka University by the Ministry of Education, Culture, Sports, Science and Technology of Japan (MEXT).

References

[1] M. Ichimiya, T. Mizuno, S. Kotake, Nucl. Eng. Technol. 39 (2007) 171.
[2] T. Namekawa, K. Kawaguchi, K. Koike, S. Haraguchi, S. Ishii, Proceeding GLOBAL Paper No. 424, 2005.
[3] Y. Sagayama, Proceeding GLOBAL, 2007, p. 251.
[4] H. Kleykamp, J. Nucl. Mater. 131 (1985) 221.
[5] H. Kleykamp, J.O. Paschoal, R. Pejsab, F. Thümmler, J. Nucl. Mater. 130 (1985) 426.
[6] R.D. Shannon, Acta Cryst. A32 (1976) 751.
[7] For example Y. Takahashi, M. Murabayashi, Y. Akimoto, T. Mukaibo, J. Nucl. Mater. 38 (1971) 303.
[8] The SGTE Pure Substance and Solution Database ver. 3.2, for use with ChemSage, GTT-Data Service (1996).
[9] K. Kurosaki, Y. Saito, H. Muta, M. Uno, S. Yamanaka, J. Alloys Compd. 381 (2004) 240.
[10] JCPDS 5-0550.
[11] A. Biancheria, Trans. Am. Nucl. Soc. 9 (1966) 15.
[12] K. Kurosaki, R. Ohshima, M. Uno, S. Yamanaka, K. Yamamoto, T. Namekawa, J. Nucl. Mater. 294 (2001) 193.
[13] S. Yamanaka, S. Yoshida, K. Kurosaki, M. Uno, K. Yamamoto, T. Namekawa, J. Alloys Compd. 327 (2001) 281.